Cell PRESS

Cancer Cell
Article

# A Critical Role for Notch Signaling in the Formation of Cholangiocellular Carcinomas

Steffen Zender,[2,8] Irina Nickeleit,[3,8] Torsten Wuestefeld,[1,8] Inga Sörensen,[5] Daniel Dauch,[1] Przemyslaw Bozko,[1] Mona El-Khatib,[1] Robert Geffers,[6] Hueseyin Bektas,[4] Michael P. Manns,[2] Achim Gossler,[3] Ludwig Wilkens,[7] Ruben Plentz,[1] Lars Zender,[1] and Nisar P. Malek[1,*]

[1]Department of Internal Medicine I, Eberhard Karls University Tübingen, Otfried-Müller-Straße 10, 72076, Tübingen, Germany
[2]Department of Gastroenterology, Hepatology and Endocrinology
[3]Institute for Molecular Biology
[4]Department of Visceral and Transplantation Surgery
[5]Department of Nephrology and Hypertension
Hannover Medical School, Carl Neuberg Strasse 1, 30625 Hannover, Germany
[6]Helmholtz Centre for Infection Research, Inhoffenstraße 7 38124 Braunschweig, Germany
[7]Institute of Pathology, Nordstadtkrankenhaus, Haltenhoffstr. 41, 30167 Hannover, Germany
[8]These authors contributed equally to this work
*Correspondence: nisar.malek@med.uni-tuebingen.de
http://dx.doi.org/10.1016/j.ccr.2013.04.019

## SUMMARY

**The incidence of cholangiocellular carcinoma (CCC) is increasing worldwide. Using a transgenic mouse model, we found that expression of the intracellular domain of Notch 1 (NICD) in mouse livers results in the formation of intrahepatic CCCs. These tumors display features of bipotential hepatic progenitor cells, indicating that intrahepatic CCC can originate from this cell type. We show that human and mouse CCCs are characterized by high expression of the cyclin E protein and identified the cyclin E gene as a direct transcriptional target of the Notch signaling pathway. Intriguingly, blocking γ-secretase activity in human CCC xenotransplants results in downregulation of cyclin E expression, induction of apoptosis, and tumor remission in vivo.**

## INTRODUCTION

Cholangiocellular carcinoma (CCC) is a primary liver cancer with biliary differentiation (Patel, 2006). Several recent studies describe a significant increase in the incidence of this tumor in Europe and the United States; the reasons for this increase are not understood (El-Serag et al., 2009; von Hahn et al., 2011; West et al., 2006). Even though CCC accounts for up to 15% of all liver cancers, the molecular alterations that lead to this disease are mostly unknown. Predisposing conditions such as primary sclerosing cholangitis, chronic infection with liver flukes, or biliary stones led to the hypothesis that chronic inflammation of the biliary epithelium might be a prerequisite for the formation of CCC. However, no uniform genetic alteration has been identified that is responsible for the formation of CCC. In addition, only very few mouse models of CCC are currently available. Recently Xu and colleagues showed that liver-specific disruption of the *SMAD4* and *PTEN* genes leads to the formation of CCC (Xu et al., 2006). NF2 knockout mice were shown to develop hepatocellular carcinomas and CCCs from a common progenitor cell (Benhamouche et al., 2010), supporting the hypothesis that CCC may arise from undifferentiated hepatic precursor cells.

A number of studies showed that the Notch signaling pathway is of central importance for embryonic development of the biliary tree. For example, loss of the Notch ligand *jagged1* or the Notch 2 gene results in congenital hypoplasia of the biliary system, called the Alagille syndrome (Geisler et al., 2008; Lorent et al., 2004; Ryan et al., 2008). Analysis of mice after liver-specific inactivation of RBP-Jκ, a common transcriptional mediator of Notch signaling, revealed a reduced number of biliary cells differentiating from hepatoblasts (Zong et al., 2009). Notch levels are regulated by ubiquitylation-dependent protein turnover, which is controlled by the $SCF^{Fbw7}$ E3-ubiquitin ligase (Welcker and Clurman, 2008). The F-Box component of this E3-ligase, the Fbw7 protein, was found to be frequently mutated in human CCC (Akhoondi et al., 2007). However, it is unknown whether Notch dysregulation is involved in the initiation and progression of CCC.

### Significance

Overactivation of the Notch signaling pathway leads to a dysregulation of the oncogene cyclin E, resulting in the formation of CCC. Inhibition of Notch activity in CCC blocks tumor cell proliferation and induces apoptosis in vitro and in vivo. Our results shed light on the pathogenesis of CCC and pinpoint Notch inhibition as a promising treatment option.

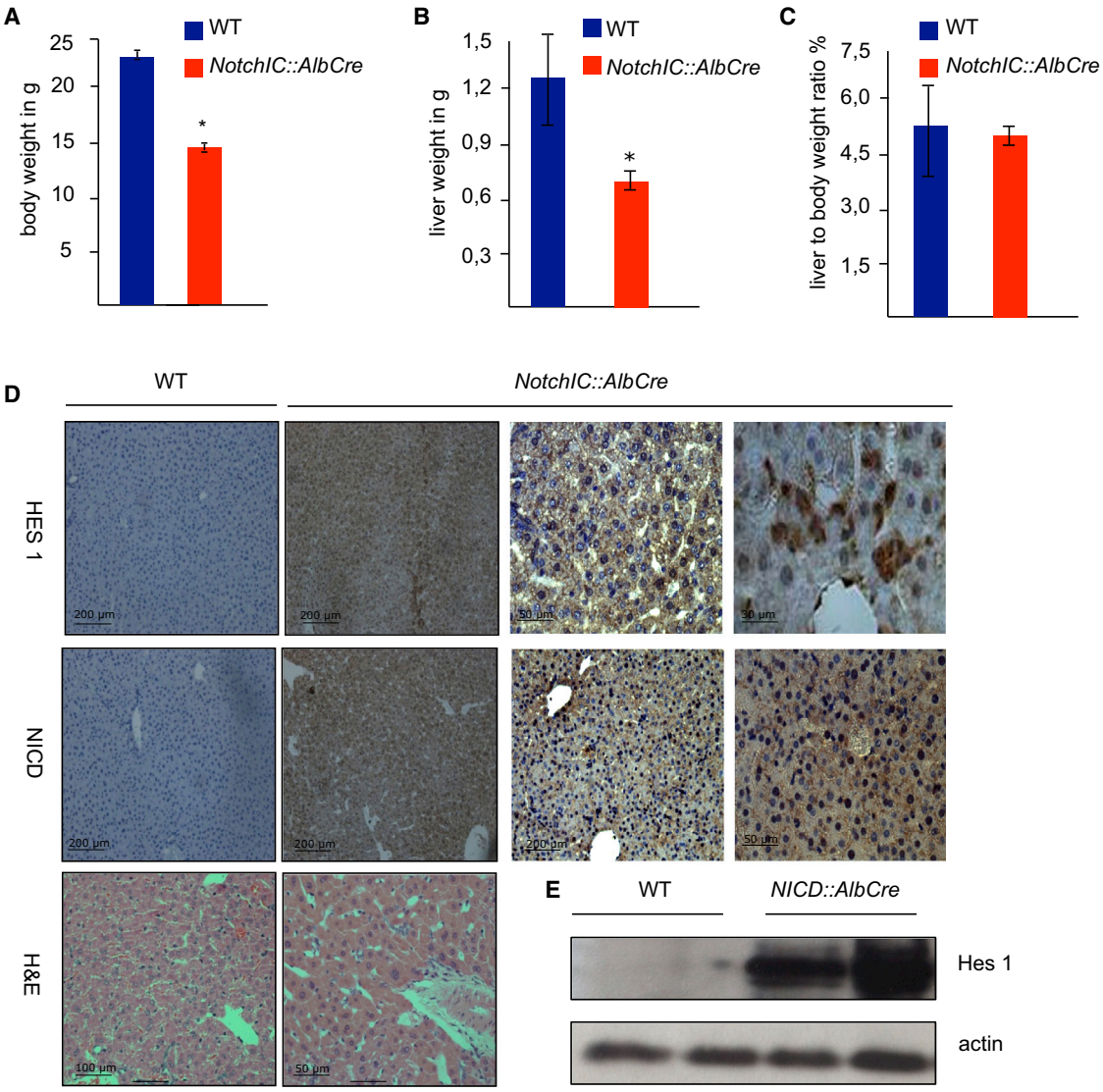


**Figure 1. *NotchIC::AlbCre* Mice Show Reduced Body and Liver Weights**

(A–C) Analysis of liver and body weight and liver-to-body weight ratio of the *NotchIC::AlbCre* mice compared to littermates (A and B: 10 weeks of age; C: 6 weeks of age).

(D) Hematoxylin and eosin (H&E) stained liver sections of *NotchIC::AlbCre* mice. Immunohistochemical staining of *NotchIC::AlbCre* livers using antibodies against Hes1 (10× and 60× magnification) and NICD in 6-week-old mice.

(E) Western blot analysis of liver tissue from two *NotchIC::AlbCre mice* and two wild-type littermates using an antibody against HES1, a downstream target of the Notch pathway in 6-week-old mice. Scale bars represent mean values ± SEM. *$p < 0.05$; **$p < 0.001$.

See also Figure S1.

In this study, we set out to explore the function of Notch signaling in the formation of liver cancers. We used a transgenic mouse line that allows the liver-specific expression of the intracellular domain of Notch receptor 1 (NICD).

## RESULTS

### Expression of Notch ICD in Mouse Liver Interferes with Hepatocyte Proliferation

To directly test the consequences of constitutive Notch expression in liver tissue, we crossed a transgenic mouse line that allows for tissue-specific overexpression of the intracellular domain of Notch 1 (*Rosa26Notch1IC*) (Murtaugh et al., 2003) to a mouse line that expresses cre-recombinase under the control of the albumin regulatory elements and the alpha-fetoprotein enhancers (AlbCre) (Kellendonk et al., 2000). Use of this cre-line results in the expression of NICD in the vast majority of all hepatocytes and biliary epithelial cells during the formation of the second ductal layer (E16.5) (Zong et al., 2009). *NotchIC::AlbCre* mice were born at normal Mendelian ratios, but showed proportionally reduced body and liver weights (Figures 1A–1C) and up to 25% reduced body size (Figure S1A [age, 7 months] available online) compared to wild-type control littermates. To show liver-specific activation of the NICD transgene,

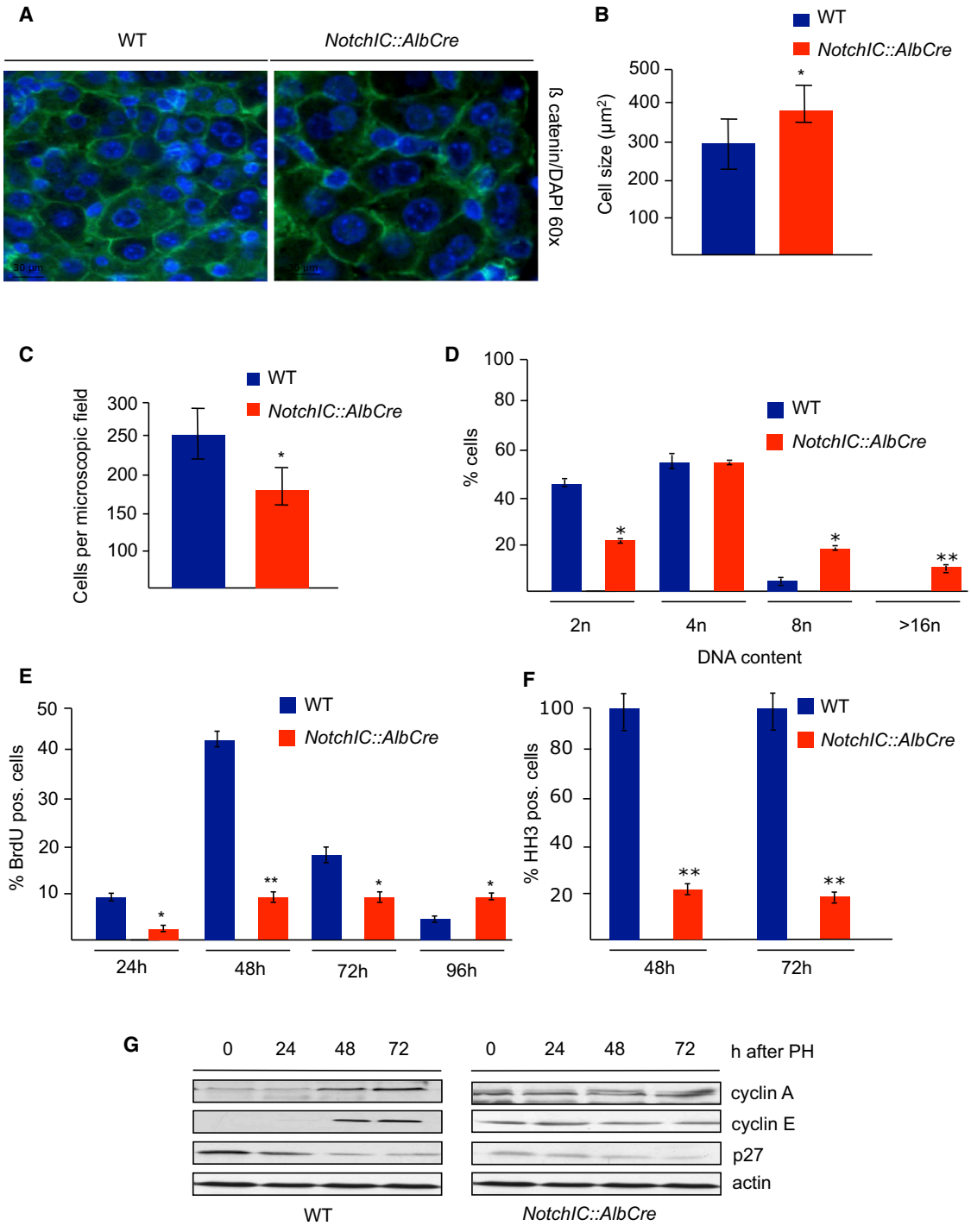


**Figure 2. Notch Signaling Leads to Dysregulated Expression of Cyclin E and Genetic Instability**

(A) β-catenin staining (for the detection of cell size) was performed on liver sections from wild-type and *NotchIC::AlbCre* mice at 12 weeks of age.

(B) Quantification of cell size in the indicated mouse strains was done after β-catenin staining to visualize the cell surface at 12 weeks of age. Five hundred cells on average were analyzed using a photometric system.

(C) Three hundred visual fields were counted on average to determine the number of hepatocytes in the livers of the indicated mouse strains at the age of 12 weeks.

(D) The DNA content of hepatocytes of the indicated mouse strains was determined by microphotometry analysis of Feulgen-stained liver sections at the age of 11 weeks.

(E and F) Quantification of the number of BrdU and phospho-Histone-H3-positive hepatocytes after induction of liver regeneration in wild-type and *NotchIC::AlbCre* double transgenic mice at the age of 10 weeks. For BrdU staining, an average of 900–2000 cells, and for HH3 staining at least 700 cells from up to

*(legend continued on next page)*

we prepared extracts from different mouse tissues and determined the expression of the green fluorescent (GFP) protein, which is co-expressed with the NICD transgene after cre-recombinase-mediated activation of transcription. As shown in Figure S1B, only the liver expressed detectable amounts of GFP, while in all other tested organs the transgene was not activated. To ensure expression and activity of the intracellular domain of Notch in cholangiocytes and hepatocytes, we performed immunostainings on mouse liver tissue from *NotchIC::AlbCre* mice and wild-type controls, using antibodies specific for the cleaved form of Notch. As shown in Figure 1D, NICD expression was detected in both cell types in the transgenic animals but not in wild-type liver controls. In line with a constitutive activation of Notch signaling, we also detected strong expression of HES1, a transcriptional target of the Notch pathway in *Notch IC::AlbCre* livers (Figure 1D) and in liver lysates (Figure 1E).

Given the expression of Notch ICD in hepatocytes and the biliary compartments of the liver, we first set out to analyze the functional consequences of Notch expression in hepatocytes. Upon histologic examination of the *NotchIC::AlbCre* liver tissues, we detected a significant increase in the cell size of the NICD-positive hepatocytes as well as variations in nuclear size in transgenic livers compared to wild-type controls (Figure 2A). Serum transaminases and different liver metabolites were also changed in *NotchIC::AlbCre* mice compared to wild-type controls (Figure S1C). To measure the size of individual hepatocytes, we stained liver sections with a specific antibody against beta catenin (Kossatz et al., 2004) and quantified the differences between *NotchIC::AlbCre* and wild-type controls (Figures 2A and 2B). In accordance with an increase in cell size, we also noticed a reduction in the number of hepatocytes per visual field in the *NotchIC::AlbCre* compared to wild-type livers (Figure 2C). Because an increase in hepatocyte size can be the result of a change in the nuclear-to-cytoplasmic ratio, we determined nuclear sizes and DNA content in *NotchIC::AlbCre* mice and wild-type control mice. As shown in Figure 2A, the nuclei of hepatocytes in *NotchIC::AlbCre* mice are significantly larger than those in control mice. To analyze if these changes were paralleled by an increase in the amount of nuclear DNA, we performed Feulgen staining and measured the DNA content of single nuclei by cytometry. As shown in Figure 2D, we found that the nuclei of hepatocytes in the *NotchIC::AlbCre* mice are not only enlarged but also contain significantly more DNA than the nuclei of nontransgenic control livers. Nuclear enlargement and an increase in DNA content are often the result of endoreduplication cycles in which the cell undergoes continuous rounds of DNA replication without cytokinesis (Kossatz et al., 2004). To test whether the *NotchIC::AlbCre* livers also display alterations with regard to cellular proliferation, we performed partial (two-thirds) hepatectomies in *NotchIC::AlbCre* transgenic animals and compared their regenerative potential with that of wild-type organs. As shown in Figure 2E, expression of *NotchIC::AlbCre* leads to an almost complete loss of regeneration potential in transgenic livers of 10-week-old mice as shown by a reduction of BrdU uptake after partial hepatectomy and a concomitant reduction in cells entering mitosis as measured by histone H3 phosphorylation (Figure 2F). This lack of proliferation was accompanied by a significant increase in hepatocyte cell size and a reduction in cell number after partial hepatectomy, thereby indicating that the *NotchIC::AlbCre* mice regenerated their liver mass through cellular hypertrophy of the remaining hepatocytes (Figure S1D). At the molecular level we found that wild-type livers downregulate the cyclin kinase inhibitor p27kip1 and started to express S phase cyclins E and A after induction of cell cycle progression by partial hepatectomy (Figure 2G). Importantly and in contrast to wild-type livers, we detected elevated levels of cyclin E and cyclin A even before partial hepatectomies were performed in *NotchIC::AlbCre* expressing livers. Together these results suggest that the expression of the intracellular domain of Notch in hepatocytes results in the induction of endoreduplication cycles and a severe impairment of cellular proliferation.

## Expression of Notch ICD in Mouse Livers Leads to the Formation of Progenitor Cell Derived Cholangiocellular Carcinomas

To understand the long-term consequences of NICD overexpression, we followed a cohort of mice for up to 15 months. In 7-month-old mouse livers, we observed areas with clusters of small cells with an epithelial appearance (Figure 3A) that also formed gland-like structures. To determine the origin of these cells, we stained liver sections with antibodies specific for the biliary tract (CK7, CK17, and CK19), hepatocytic markers (CK8/18), and the stem cell marker CD34. As shown in Figure 3A, the small epithelial cells stained positive for biliary-hepatocytic as well as stem cell markers, a finding which is typical for cells that show characteristics of hepatocytic and cholangiocytic differentiation. Such cells often arise through the transformation of bipotential hepatic progenitor cells (Kim et al., 2004), which are located in the canals of Hering.

Importantly, as early as 8 months after birth we started to observe changes in nuclear morphology in primary liver tissues from *NotchIC::AlbCre* mice. To test whether the observed cells were indeed tumor cells, we transplanted primary tissue from *NotchIC::AlbCre* mouse livers subcutaneously on the flanks of immunodeficient mice. All implantations resulted in the formation of tumors. Figure 3B shows the growth curve of the subcutaneous tumors that arose after cell transplantation. Histopathologic analysis revealed that these tumors show many features of human CCCs (Figure 3C), including the expression of CK7 and CK17 and a typical desmoid reaction of the surrounding tissue. Liver tissue from *Alb-Cre* mice was used as a control and did not give rise to tumors (Figure S2G). These results suggested that intrahepatic expression of NICD in hepatic progenitor cells can induce differentiation of these cells toward the biliary lineage and that, over time, NICD expression induces malignant transformation of these cells. To directly test this hypothesis, we

six mice per time point were counted. The average number of HH3-positive cells in the wild-type mouse was set as 100%. The number of HH3-positive cells in *NotchIC::AlbCre* mice is displayed relative to the number of HH3-positive cells in the wild-type mice.
(G) Analysis of the expression levels of cyclin A, cyclin E, p27, and actin in liver tissue lysates at the indicated time points after induction of liver regeneration in the indicated mouse strains at the age of 10 weeks.
Scale bars represent mean values ± SEM. *$p < 0.05$; **$p < 0.001$.

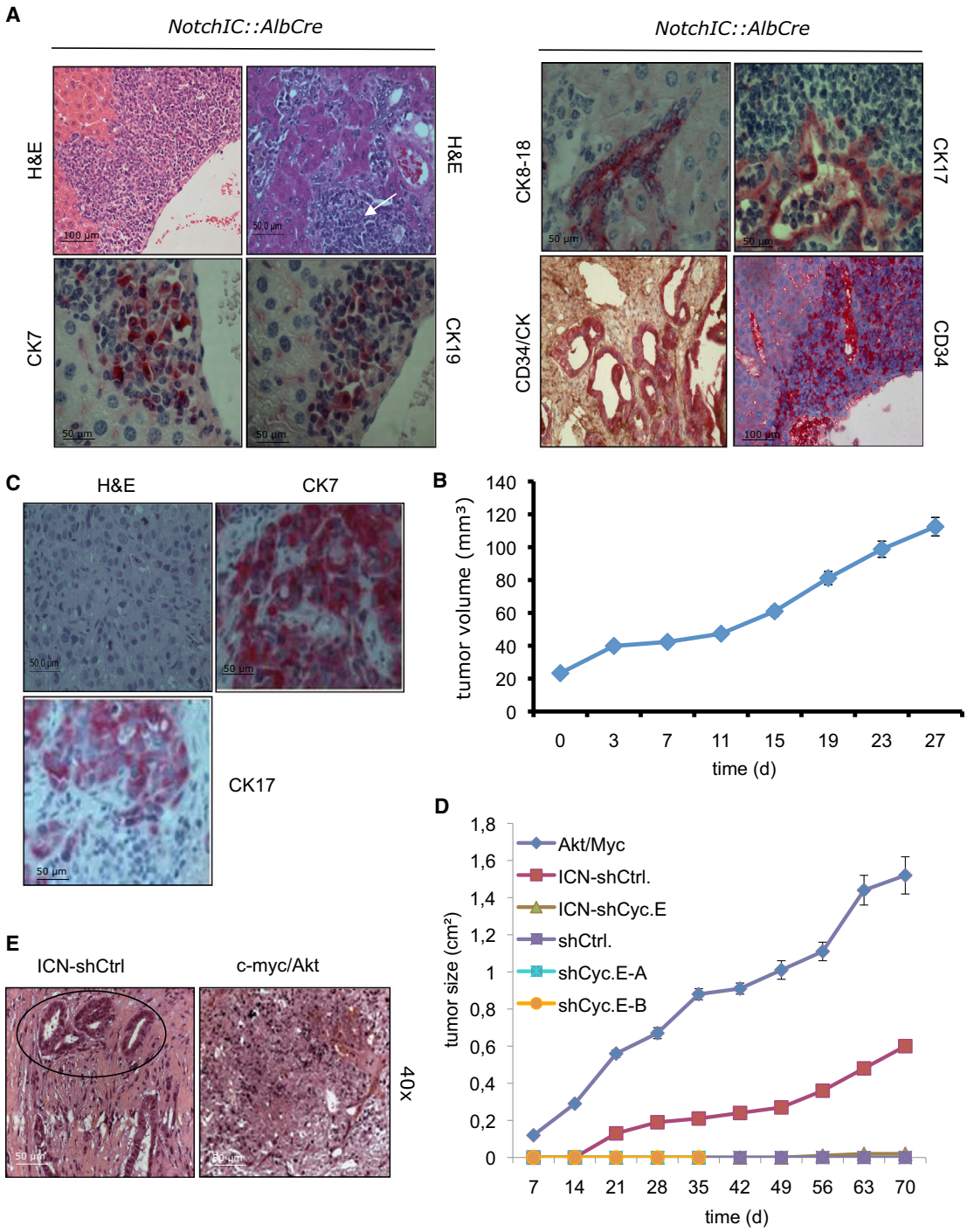


**Figure 3. Expression of Notch ICD in Mouse Liver Leads to Formation of Progenitor Cell Derived Cholangiocellular Carcinomas**

(A) H&E stained liver sections of *NICD:AlbCre* mice. Immunohistochemical staining of *NotchIC::AlbCre* livers at the age of nine months using antibodies against CK7, CK19, CK17, CK8-18, CD34, and CD34/Cytokeratin double staining.

(B) *NotchIC::Alb Cre* livers at the age of 9 months were minced and injected subcutaneously into nude mice. The growth of the resulting tumors was monitored.

(C) H&E and immunohistochemical analysis of the explanted tumor tissue using CK7 and CK17 antibodies 3 weeks after implantation of tumor cells.

(D) Growth curves of tumors after s.c. injection of progenitor cells of the indicated genotypes: progenitor cells expressing c-Myc and Akt, progenitor cells expressing the intracellular domain of notch and a control shRNA (ICN-shCtrl.), progenitor cells expressing ICN together with a shRNA targeting cyclin E (ICN-shCyc.E), progenitors that only express shRNA control (shCtrl.), and progenitor cells expressing only shRNAs that target cyclin E (shCyc.E-A/B).

(E) H&E stained tissue derived from subcutaneously growing tumors that originated from NICD expressing bipotential progenitors either transduced with ICN (ICN) and a shRNA control (ICN-shCtrl) or with Myc/Akt. The circle indicates atypical fused glands with hyperchromatic and irregular nuclei growing in a desmoplastic stroma. See also Figure S2.

infected previously described mouse bipotential liver progenitor cells (Zender et al., 2006) with retroviral vectors to stably overexpress the intracellular domain of Notch. Vector-infected cells served as controls. Figure S2A shows the expression levels of NICD in such cells compared to empty vector-infected cells. Cells stably expressing NICD were subcutaneously injected into nude mice and tumor growth was analyzed over time. While control vector-transduced cells did not give rise to tumors, NICD-overexpressing cells formed subcutaneous tumors (Figure 3D) in all transplantation experiments. These tumors showed all features of CCCs (Figure 3E). Interestingly, tumors arising from progenitor cells stably transduced with c-Myc and a constitutive active form of Akt showed a different histopathology and were classified as undifferentiated hepatocellular carcinomas/hepatoblastomas (Figure 3E). These results indicate that expression of the intracellular domain of Notch leads to tumor formation in all transgenic mice and can transform hepatic progenitor cells thereby leading to the development of CCCs.

## Notch Signaling Leads to Dysregulated Expression of Cyclin E and Genetic Instability

To understand the molecular pathogenesis of Notch-dependent CCC formation, we focused our analysis on the function of the cyclin E protein. As shown in Figure 2G, cyclin E is highly expressed in *NotchIC::AlbCre*-derived liver tissue even before the onset of liver regeneration (time point 0). In line with this finding, we detected high levels of cyclin E protein within the CCCs derived from *NotchIC::AlbCre* mice (Figure 4A). Previous studies on the oncogenic function of cyclin E suggested that cyclin E induces DNA damage, thus resulting in genetic instability and contributing to the formation of malignant tumors (Spruck et al., 1999). We therefore tested if cyclin E-overexpressing cholangiocellular tumors might show signs of DNA damage by staining primary mouse CCC tissues derived from *NotchIC::AlbCre* mice with antibodies specific for the phosphorylated form of Ser-139 of histone H2AX (γH2AX), a marker for DNA double-strand breaks. As shown in Figure 4B, we found that more than 70% of all cells in these CCCs show signs of DNA damage as compared to wild-type liver tissue. Similarly, tumor tissues derived from nude mice transplanted with primary tumor cells from *NotchIC::AlbCre* also showed high levels of cyclin E expression and stained positive for γH2AX (Figure 4C). Mice expressing only cre-recombinase do not show any signs of genetic instability as measured by γH2AX staining (Kossatz et al., 2010). We then determined whether a reduction in cyclin E expression would reduce the number of γH2AX-positive cells. Figure 4D shows that transfection of human MzChA1 cholangiocarcinoma cells with siRNAs against cyclins E1 and E2 (Figure S2B) led to a significant reduction in the number of γH2AX-positive cells.

Based on these results, we speculated that Notch signaling might be directly involved in the regulation of the cyclin E promoter and thus in the induction of genetic instability and CCC initiation and progression. Interestingly, the cyclin E1 promoter contains several Rbpjκ binding sites that could be involved in the regulation of the promoter by NICD signaling. We used a previously described cyclin E1 promoter luciferase reporter construct (Geng et al., 1996) to measure promoter activity in the CCC cell with or without NICD overexpression. To determine the activity of the cyclin E gene, we transfected the CycE-Luc promoter construct into CCC cells (MzChA1, TFK1) and measured luciferase expression in these cells as compared to that in hepatocellular carcinoma cell lines (Hep3B, HepG2). As shown in Figure 4E, we found higher basal levels of cyclin E promoter activity in the CCC cell lines as compared to levels in liver cancer cells (Hep3B) or hepatoblastoma cells (HepG2). Next, we determined whether NICD was able to induce the activation of the cyclin E promoter. Cotransfection of NICD with the CycE-Luc reporter construct resulted in a more than 10-fold induction of the cyclin E promoter (Figure 4E). Moreover, cotransfection of NICD with an expression plasmid for the dominant-negative co-activator Mastermind prevented the activation of the cyclin E promoter by NICD, indicating that the activation of the cyclin E promoter was a direct consequence of NICD activity.

Given the importance of cyclin E expression for the generation of genetically unstable CCC cells, we next tested whether the induction of cyclin E is required for the observed oncogenic transformation of bipotential hepatic progenitors. For this purpose, we transduced NICD-expressing liver progenitor cells with retroviruses for stable expression of two different shRNAs against cyclin E. After selection, we measured the knockdown level of cyclin E in these cell populations (Figures S2C and S2D) and transplanted these cells subcutaneously into immunodeficient mice. As shown in Figure 3D, compared to ICN-expressing cells that were transduced with control shRNAs, there was a strong inhibition of tumor development from cells with stable expression of cyclin E shRNAs together with ICN. Overall, only one mice developed tumors (mouse 1a,1b). Western blot analysis of the tumor tissue showed profound cyclin E protein expression (Figure S2E), indicating a selection against RNAi-mediated cyclin E knockdown in these particular tumors. Our results suggest that expression of NICD results in the activation of the cyclin E promoter and increased cyclin E expression which, through the induction of genetic instability, leads to the formation of CCCs.

## Notch 1 and 3 Are Overexpressed in Human Cholangiocellular Carcinoma

Prompted by these results, we next tested whether the Notch pathway is also active in human CCC cells and tissues. We first determined the expression and activity of the Notch signaling pathway in three established human CCC cell lines (TFK1, MzChA1, and EgI1) and also in a primary cell line that we derived from a CCC tumor specimen (SZ1). As shown in Figure 5A, all CCC cell lines expressed the Notch1 receptor as well as the Notch ligand jagged while hepatocellular or colon carcinoma cell lines did not show an activation of this pathway (Figure S2F). To determine whether the Notch signaling pathway is active in CCC cells, we used an antibody that recognizes the cleaved form of Notch 1 (Notch val 1744) and the downstream target gene *Hes1*. As shown in Figure 5A, all CCC cell lines expressed the activated form of the Notch receptor and the HES1 protein, indicating that the Notch signaling pathway is active in these tumor cells but not in HeLa cells, which we used as a control. To ensure that the NICD transgenic mouse line is an adequate model system, we compared the expression levels of NICD in the CCCs that arose in our transgenic animals to the levels expressed in the human CCC cell lines. As shown in Figure 5B, mouse tissue and human CCC lines express comparable levels of cleaved Notch and HES1 protein. Finally, we tested whether

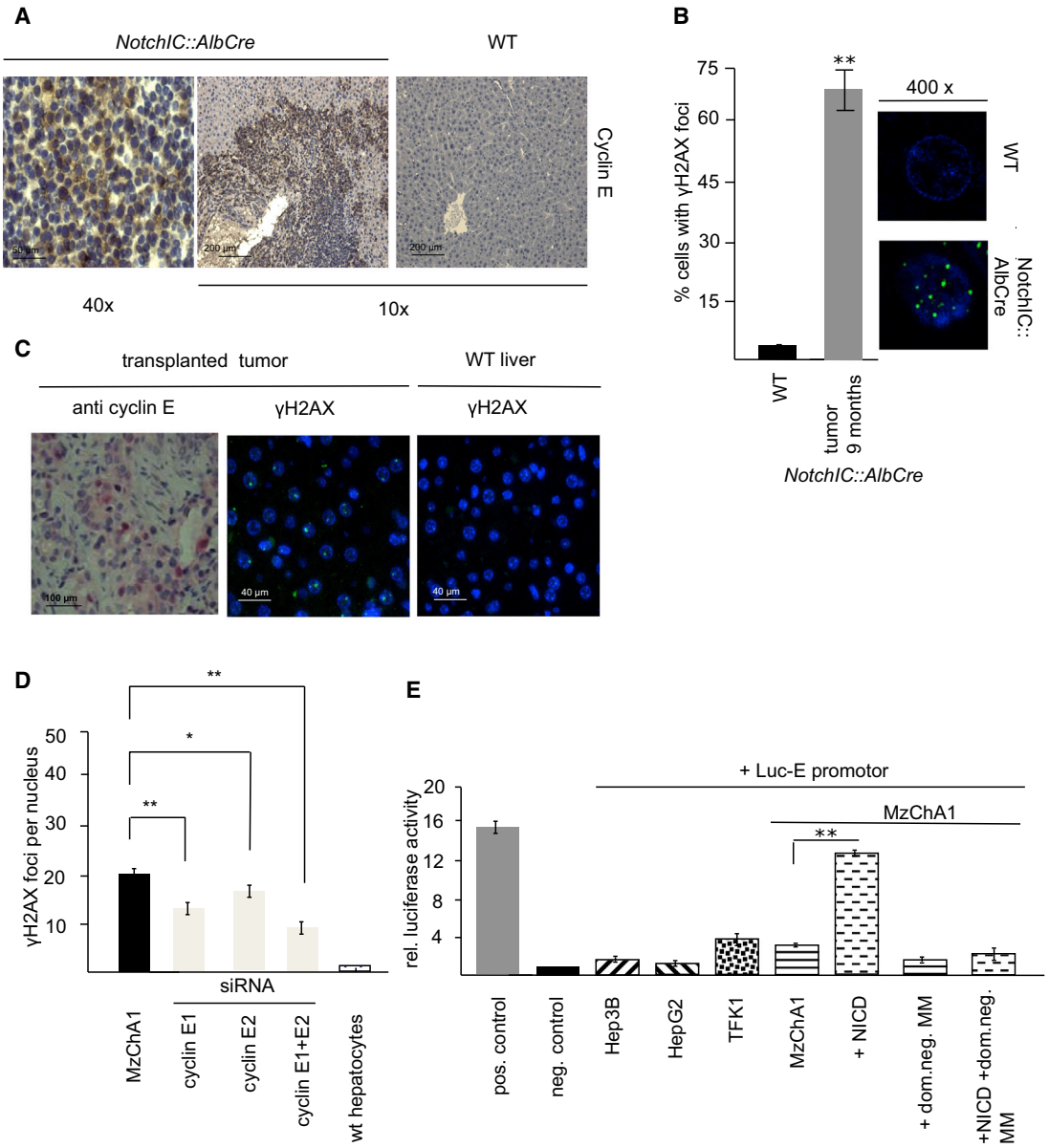


**Figure 4. Notch Signaling Leads to the Transformation of Bipotential Hepatic Progenitors through Dysregulation of Cyclin E Expression**

(A) Immunohistochemical staining of wild-type and *NotchIC::AlbCre* livers at the age of 9 months using a cyclin E antibody.

(B) Livers from wild-type controls or tumor tissue derived from 9-month-old *NotchIC::AlbCre* mice were stained with a γH2AX antibody to determine the number of nuclei that showed signs of DNA damage. The plot shows the staining results of at least 300 cells per mouse strain. An example of *NotchIC::AlbCre* and wild-type nuclei is shown in a 400× magnification on the right side.

(C) Representative examples of γH2AX and cyclin E stained transplanted mouse CCCs and wild-type liver control.

(D) Statistical analysis of γH2AX foci in MzChA1 cells and after depletion of cyclin E expression through siRNA-mediated knockdown of cyclin E1, cyclin E2, or both.

(E) MzChA1, TFK1, Hep3B, and HepG2 cells were transfected with the indicated plasmids and relative luciferase activity was measured after 48 hr. Scale bars represent mean values ± SEM. *$p < 0.05$; **$p < 0.001$.

the activation of the Notch pathway is involved in the pathogenesis of human CCC. We determined the expression levels of the Notch receptors (Notch 1, 2, 3, and 4) in 56 primary CCC tumor tissues (see Table S1 for details) with immunohistochemical staining. As shown in Figure 5C and in the diagram in Figure 5D, we found that the majority of all CCCs overexpress the Notch 1 receptor. Additionally, we found a strong overexpression of the Notch 3 receptor in primary tumor tissue as compared to that in wild-type liver tissue. For both types of receptors, we detected a predominant nuclear staining, whereas normal liver tissue did not stain positive for either receptor (Figures S3A and S3B). Finally, we tested the expression of the cyclin E protein in our collection of primary human CCC tissues. As shown in Figures 5E and S3C, we found a strong or very strong expression of the

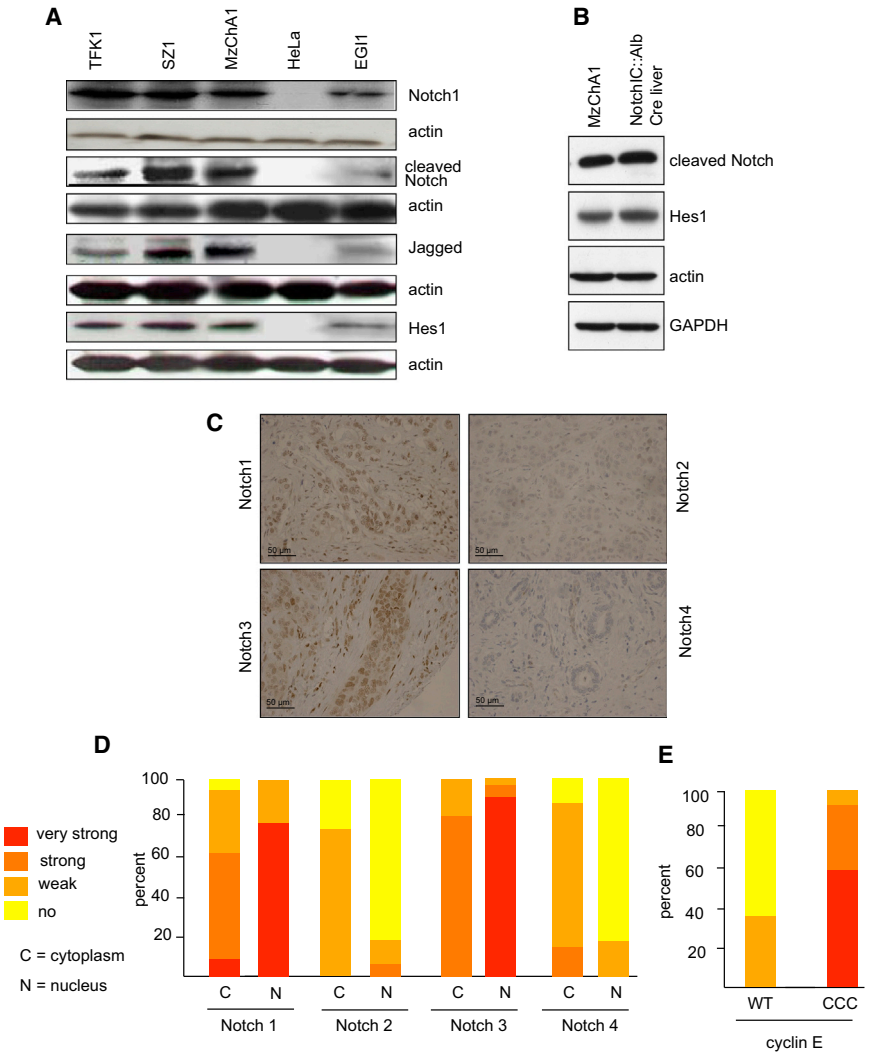


**Figure 5. The Notch Signaling Pathway Is Activated in Human CCC**

(A) TFK1, MzChA1, EGI1 cells, a CCC primary culture (SZ1), and HeLa cells were lysed and the expression levels of Notch 1, cleaved Notch, Jagged 1 and HES1 were analyzed by western blotting.

(B) Comparison of cleaved Notch and HES1 levels in human CCC cell lines and tumor tissue derived from *NotchIC::AlbCre* mice. Actin and GAPDH were used as loading controls.

(C) Fifty-six different human CCCs were screened for Notch 1, 2, 3, or 4 expression using a tissue microarray.

(D) Analysis of the staining intensities of the tissue microarray displayed is the percentage of tumors that express the Notch receptors 1–4 in the cytoplasm as well as in the nucleus in the 56 CCC samples tested.

(E) Immunohistochemical analysis of 56 human CCCs shows a strong expression of cyclin E1 compared to wild-type livers.

See also Figure S3 and Table S1.

cyclin E protein in the majority of all CCC samples tested. Because our analysis of the cyclin E promoter suggested that cyclin E is a transcriptional target of Notch signaling, we tested whether Notch and cyclin E expression correlate in primary CCC tissues. Using the Kendall tau-b rank test, we found that cyclin E1 and Notch 1 showed a highly significant ($p < 0.001$) co-expression in the CCC tissues tested. These results suggest that overexpression of Notch promotes the expression of the cyclin E gene through activation of the cyclin E promoter, which results in the formation of DNA double-strand breaks in human CCC cells.

## Notch Signaling as a Therapeutic Target in CCC

Our analysis of primary CCC tissues and the observation that NICD transgenic mice develop CCCs point toward a central role of the Notch signaling pathway in the formation of these tumors. To test whether the expression of Notch was also required for CCC maintenance, we transfected the cells with siRNAs specific for Notch 1. As shown in Figure 6A, loss of Notch 1 expression led to a reduction in HES1 and cyclin E expression while p53, p27, and p21 were strongly induced. Forty-eight hours after the transfection of Notch 1 siRNA, approximately 50% of all MzChA1 cells had undergone apoptosis (Figure 6B). Combined ablation of Notch 1 and 3 by siRNA led to an even more pronounced effect, indicating that signaling through both receptors is required for CCC maintenance (Figures S4A and S4B).

Notch signaling depends on γ-secretase-mediated generation of NICD, which translocates to the nucleus to induce a cell type-specific transcriptional program. To test whether γ-secretase inhibition of Notch signaling might constitute a treatment option against CCC, we treated these cells with the γ-secretase inhibitor N-[N-(3,5-difluorophenacetyl)-L-alanyl]-S-phenylglycine t-butyl ester (DAPT). As shown in Figure 6C, DAPT treatment resulted in a time-dependent decrease in the expression of the cleaved form of the Notch receptor and the Notch target gene *Hes1*. Similar results were obtained with other CCC cell lines (Figure S4C). In line with our observation that Notch controls cyclin E transcription, DAPT treatment also led to a decrease in cyclin E expression in MzChA1 cells as determined by RT-PCR (Figure S4D). To determine the functional consequences of Notch inhibition, we determined the number of apoptotic MzChA1 cells after treatment with DAPT. As shown in Figure 6D, DAPT treatment of MzChA1 cells resulted in a significant increase in the number of apoptotic cells as measured by the activation of caspases 3 and 7. This decrease in viability was accompanied by a significant reduction of BrdU uptake (Figure S4E) and a strong increase in the expression levels of the cyclin kinase inhibitors p21 and p27 as well as the tumor suppressor protein p53 (Figure S4F). Similar results were found in the other CCC lines (EGI-1, TFK-1) (data not shown).

Finally, we tested whether inhibition of Notch signaling would also affect the growth of xenotransplanted human CCCs. To this

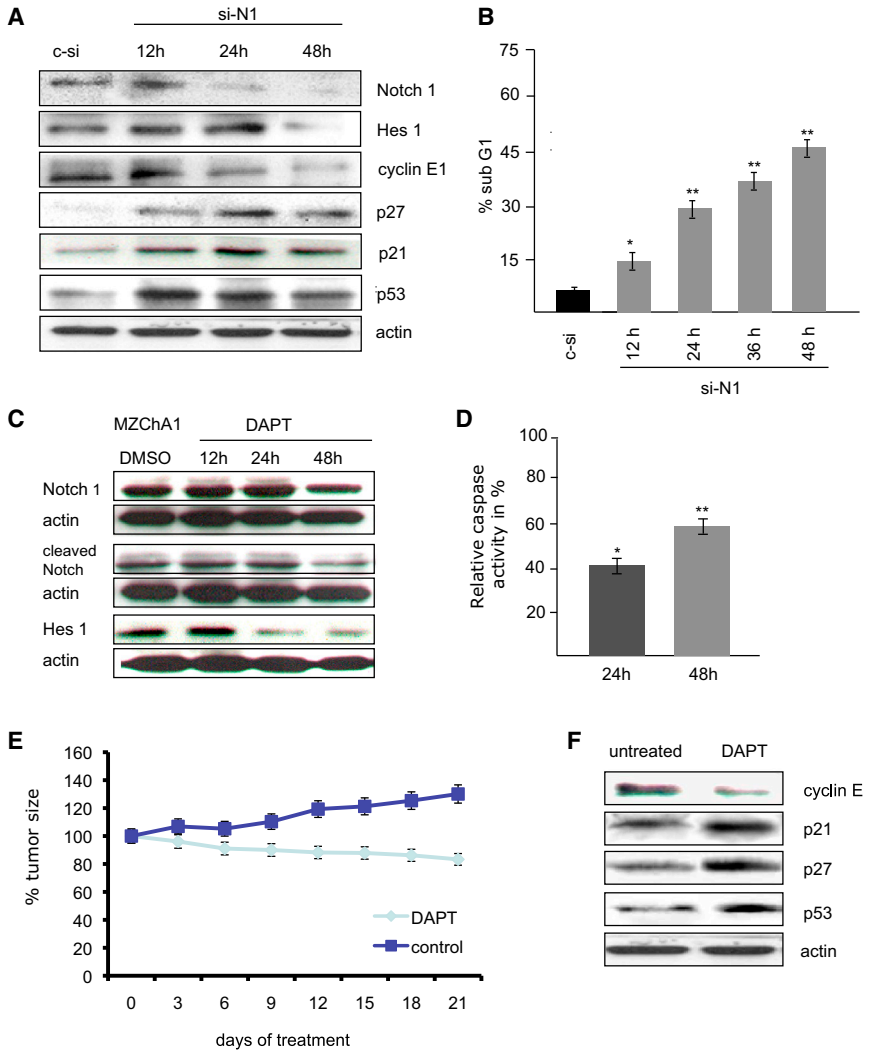


**Figure 6. Notch Signaling as a Therapeutic Target in CCC**

(A) Western blot expression analysis of Notch 1, HES1, cyclin E, p21, p53, and p27 after siRNA-mediated knockdown of Notch 1 in MzChA1 cells.

(B) Determination of cell death (sub G1 fraction) by FACS scan analysis in MzChA1 cells in which Notch1 expression was reduced through siRNA-mediated knockdown.

(C) MzChA1 cells were treated with DAPT (10 μM) for the indicated periods of time. At different time points cells were lysed and the expression levels of Notch 1, cleaved Notch 1, and HES1 were analyzed by western blotting.

(D) Caspase 3/7 activity in DAPT-treated MzChA1 cells at the indicated time points. The y-axis describes the relative caspase activity in percentages as compared to the DMSO control treated cells.

(E) Primary human CCC cells (SZ1) were transplanted under the skin of nu/nu mice (ten mice for each group). When the tumors reached a size of approximately 150–200 $mm^3$, mice were treated with DAPT at a concentration of 50 mg/kg every 72 hr or with DMSO, which was used to dissolve DAPT (control).

(F) Western blot analysis of the expression levels of cyclin E1, p21, p27, p53, and actin in tumor tissue lysates from DAPT treated or untreated mice. Scale bars represent mean values ± SEM.

See also Figure S4.

in growth factor signaling have been described. Nevertheless, treatment options are still sparse and given the lack of a detailed understanding of the underlying pathogenesis, targeted therapies are difficult to implement. In this study, we used a transgenic mouse line that expresses the intracellular domain of the Notch 1 receptor in liver cells starting at day 9.5.

end, we established primary CCC cell lines from human CCCs that were resected at our institution. Cells derived from cell line SZ1 were mixed with Matrigel and injected subcutaneously into immunodeficient mice. When the tumors reached a size of approximately 150–200 $mm^3$, mice were treated with DAPT at a concentration of 50 mg/kg every 72 hr. As shown in Figure 6E and Figure S4G, inhibition of γ-secretase resulted in a significant inhibition of tumor growth as compared to untreated controls. This inhibition of tumor growth was accompanied by the induction of p21, p27, and p53 and a downregulation of cyclin E expression in the primary tumor tissues (Figure 6F). Histologic examination of these tumors revealed, in accordance with the results we had obtained using CCC cell lines, that treatment with DAPT resulted in the induction of apoptosis in the xenotransplanted tumors as shown by TUNEL staining of the primary tissues (Figure S4H).

## DISCUSSION

The pathogenesis of CCC is only incompletely understood. A number of genetic and epigenetic changes as well as alterations

Our phenotypic and molecular analysis of the *NotchIC::AlbCre* mice revealed opposite roles for Notch signaling in the hepatic and cholangiocytic compartments. We found that NICD-overexpressing hepatocytes undergo endoreduplication cycles that result in the formation of polyploid liver cells. This defect in mitotic cell division is also apparent in liver regeneration experiments that show that NICD-expressing hepatocytes fail to reenter the cell cycle after a partial hepatectomy. In line with our findings Croquelois and colleagues showed that loss of Notch 1 in hepatocytes led to the overproliferation of hepatocytes, which caused the formation of regenerative nodules (Croquelois et al., 2005). Together, these results suggest that Notch signaling in hepatocytes is primarily antiproliferative and prevents uncontrolled proliferation of liver cells.

We found that overexpression of NICD results in the formation of CCCs, implicating this signaling pathway in the pathogenesis of this tumor. Zong and colleagues convincingly showed that ectopic Notch expression led to the formation of biliary epithelial cells in the hepatic lobule (Zong et al., 2009). Moreover, expression of Notch in livers of 6-day-old mice led to the formation of ectopic biliary structures within the liver. Their experiments

therefore argue for the ability of Notch signaling to induce a fate decision in hepatoblasts or even terminally differentiated hepatocytes that allows them to differentiate toward the biliary lineage. The ability of hepatocytes to change their fate decision under the influence of AKT and Notch signaling or under conditions of chemically induced carcinogenesis has been shown recently (Fan et al., 2012; Sekiya and Suzuki, 2012). These studies provided evidence that hepatocytes localized around the central vein can be transformed into biliary cancers. While a growing body of evidence supports the hypothesis that human CCC is derived from intrahepatic stem cell compartments (Cardinale et al., 2012; Nakanuma et al., 2010), it needs to be shown whether a change in cellular differentiation can contribute to human CCC pathogenesis. Recent data in other systems indicate that Notch signaling drives intestinal cell fate determination of progenitor cells, for example, those lining the intestinal crypts, and blockade of Notch signaling via gamma secretase inhibition forces intestinal progenitor cells to differentiate into goblet cells (van Es et al., 2005; Zecchini et al., 2005). This pathologic profile is reminiscent of that seen in *Hes-1* deficient mice, a downstream Notch target gene (Kodama et al., 2004). Our analysis showed that expression of NICD in mouse liver cells results in the formation of CCCs, which in addition to cholangiocytic features, also express surface markers associated with stem cells thereby indicating that NICD expression in undifferentiated liver progenitor cells might have transformed those cells into tumor cells. It is not known how the expression of Notch ICD in differentiated cholangiocytes may also result in the formation of cancers.

The finding that NICD expression in hepatic progenitors results in the formation of CCCs was further substantiated by the fact that cells isolated from these primary tumors led to the formation of CCC after transplantation into nude mice. Given the high plasticity of these cells, we cannot exclude that Notch signaling might lead to the formation of tumors that resemble features of hepatocellular carcinoma or even mixed phenotypes (Villanueva et al., 2012). We therefore set out to directly prove that aberrant Notch signaling in bipotential liver progenitor cells causes the formation of CCC. To this end, we created progenitor cell lines that stably express NICD and found that these cells did indeed start to form tumors that show all characteristics of CCCs after transplantation into mice. These tumors also showed elevated levels of cyclin E expression and a high degree of genetic instability. We therefore concluded that liver progenitor cells can act as the cells of origin in the formation of CCCs in response to Notch signaling.

A central question that arose out of these findings is how the expression of NICD can lead to the formation of CCC. In this work, we found that cyclin E protein levels are greatly increased not only in CCCs derived from *NotchIC::AlbCre* mice, but also in primary human CCC tissues. Several mouse models have demonstrated that deregulated cyclin E expression is causally associated with tumorigenesis in vivo. Overexpression of human cyclin E in mammary or thymic tissues, or prevention of cyclin E degradation through mutation of the T380 phosphorylation site in mouse cyclin E, resulted in the formation of tumors (Hwang and Clurman, 2005; Loeb et al., 2005). The oncogenic function of cyclin E is coupled to its ability to induce double-strand breaks that ultimately result in the formation of genetically unstable cells. Using γH2AX as a marker for double-strand breaks, we showed that the tumors derived from *NotchIC::AlbCre* mice as well as tumors derived from NICD-expressing bipotential progenitors show high levels of DNA double-strand breaks and that reduction of cyclin E expression ameliorates this phenotype. Interestingly the dysregulation of cyclin E expression is caused by an increased transcription of the cyclin E promoter in response to NICD expression a finding that defines cyclin E as a direct transcriptional target of the Notch signaling pathway. Given that suppression of cyclin E expression by shRNA treatment results in a complete suppression of tumor formation in NICD-expressing liver progenitors, we conclude that cyclin E is indeed a critical downstream effector of Notch signaling-induced tumor formation.

Our observations together with the data provided by Zong and Stanger therefore suggest that Notch signaling can induce a biliary differentiation program in hepatocytes or hepatic progenitor cells, which together with the aberrant expression of the cyclin E protein results in the formation of intrahepatic CCCs. It is currently unknown why the Notch 1 and 3 receptors are upregulated in CCC cells. T cell acute lymphoblastic leukemia, breast cancer, and other tumors or cell lines derived from such cancers show genetic alterations that affect the expression of different components of the Notch signaling pathway (Koch and Radtke, 2007).

Recently, Fbw7, the F-Box protein that controls the turnover of Notch 1 as part of a $SCF^{Fbw7}$ ubiquitin ligase, was shown to be mutated in up to 35% of all CCCs examined (Akhoondi et al., 2007). This result points to a defect in Notch turnover that might contribute to the increase in protein levels. Interestingly the $SCF^{Fbw7}$ complex also ubiquitylates the cyclin E1 and E2 proteins and loss or mutation of the Fbw7 protein results in increased cyclin E expression (Koepp et al., 2001; Welcker et al., 2003). We have shown that overexpression of the Notch ICD in mouse livers leads to an increase in cyclin E expression and that Notch ICD can directly transactivate the cyclin E1 promoter. Loss of Fbw7 might therefore cause an increase in cyclin E levels not only through a reduction of cyclin E ubiquitylation and turnover, but also through an increased transcription of the Cyclin E gene through the Notch signaling pathway.

CCCs frequently arise under conditions of chronic inflammation. The interleukin-6 (IL-6)/gp130 signaling system constitutes an important component of the inflammatory response in the liver and was shown to be involved in the pathogenesis of CCCs. This aberrant overexpression of IL-6 is a consequence of the epigenetic silencing of the suppressor of cytokine signaling 3 (SOCS-3) (Isomoto et al., 2007). Intriguingly IL-6 is able to induce a Notch-3–dependent transcriptional activation of the jagged gene in breast cancer cells (Sansone et al., 2007). Dysregulation of Notch signaling might therefore be a result of alterations in its proteolytic turnover and exogenous factors like the stimulation of jagged transcription by IL-6. While this hypothesis awaits experimental proof, our experiments using isolated NICD-expressing progenitors show that transformation of these cells does not require additional inflammation.

To date, no specific treatment exists for patients with CCCs that are not eligible for surgery. We therefore set out to test whether inhibition of Notch signaling would interfere with the proliferation and survival of CCC cells. Loss of Notch signaling either by inhibition of γ-secretase or by suppressing Notch

activity through siRNA-mediated ablation of Notch 1 and 3 expression resulted in the induction of cell cycle arrest and apoptosis. Notch inhibition also led to the regression of established xenotransplant tumors derived from CCC cell lines in vivo. Inhibition of γ-secretase activity might therefore constitute a molecular target that interferes with the dysregulated expression of cyclin E.

In this study we found that *NotchIC::AlbCre* mice not only formed ectopic biliary structures, but also intrahepatic CCCs. Together with the observation that Notch can induce a biliary cell fate in bipotential progenitors lead to the idea that the pathogenesis of intrahepatic CCCs might differ significantly from the formation of biliary tumors that arise primarily from the bile ducts (i.e., Klatskin carcinoma). Our data suggest that intrahepatic CCC might constitute a tumor that forms as a result of aberrant Notch signaling in hepatic progenitors that transform into tumor cells. Moreover we show that inhibition of Notch signaling constitutes an attractive target for future clinical trials in patients with intrahepatic CCCs.

## EXPERIMENTAL PROCEDURES

### Animals and Partial Hepatectomy Procedures

*ROSA26 NICD* mice (Murtaugh et al., 2003) were crossed with *AlbCre* mice (Kellendonk et al., 2000) to generate mice with a liver-specific overexpression of the activated form of the Notch 1 receptor. All genotyping was performed as described (Murtaugh et al., 2003). In all experiments, 8- to 10-week-old wild-type and double transgenic littermates were used. Mice were killed at the indicated time points after surgery, and the number of mice analyzed ranged from five to six per time point. Partial hepatectomy was performed as described (Satyanarayana et al., 2003). All animal experiments were performed after review and approval by the Niedersächsische Landesamt für Verbraucherschutz und Lebensmittelsicherheit, Lower Saxony, Germany.

### Immunohistochemical Staining of Mouse and Human Tissues

Immunohistochemical staining of mouse and human tissue was performed as described previously (Kossatz et al., 2004). Surgical specimens were taken for diagnostic and scientific purposes permitted by the Ethics Committee of the University of Bern, Switzerland. Informed consent was obtained from all patients.

### Feulgen Staining

To determine the DNA content, 3 μm sections were Feulgen-stained using the Feulgen Staining Kit (Merck). Ploidy analysis was performed with the Ahrens ICM, Cytometric System. Statistical analysis was done using the Dunnett t test (DNA ploidy) and the mixed models analysis of variance (nuclear size analysis).

### RT-PCR

RNA extraction was done as described (Satyanarayana et al., 2003). For cDNA synthesis, 2 μg of RNA were used. The RT reaction was carried out using SuperScript-II RNase H reverse transcriptase (Invitrogen). For semiquantitive RT-PCR, 1 μl cDNA was amplified using the following cycles: denaturation 94°C for 30 s, annealing 57°C for 1 min, and extension 72°C for 45 s using RedTaq (Sigma) for 35 cycles. Actin was used as a control.

### siRNA

siRNA knockdown was performed using FuGene6 transfection reagent. Transfections were performed using siRNA at a concentration of 20 nM for Notch 1 si RNA; sc-36095 and Notch 3 siRNA; sc-37135 from Santa Cruz. siRNA in a concentration of 40 nM was used for cyclin E1 and cyclin E2 knockdown.

### DAPT Treatment In Vitro

Five milligrams of DAPT were dissolved in 1 ml dimethyl sulfoxide. Cells were plated in six-well plates. When the cells reached 60% confluency, they were treated with 38.7 μM DAPT. Cells were collected after 12, 24, 36, and 48 hr for protein extraction and analyzed by western blot.

### Western Blot

Antibodies included cleaved Notch 1 (Val1744, Cell signaling); Hes-1 (Santa Cruz Biotechnology); Notch 1: C-20; sc 6014 (Santa Cruz), Notch 3: (M-134); sc5593 (Santa Cruz); Jagged 1:C-20, sc-6011 (Santa Cruz); p27: Cat 610242 (BD Transduction), p21 C-19; sc397 (Santa Cruz), p53 FL-393, sc6243 (Santa Cruz); and cyclin E: C19 (Delta Biolabs). Western blots were performed as described (Malek et al., 2001).

### Generation of Immortalized Bipotential Liver Progenitor Cells, Retroviral Transduction, and Subcutaneous Injection of Cells

Bipotential liver progenitor cells were isolated from C57Bl6 embryonic mouse livers as described recently (Zender et al., 2006). For additional information, please refer to the Supplemental Experimental Procedures.

### Statistical Analysis

Statistical analysis was carried out using Microsoft Excel software. Unless stated otherwise, all data are presented as mean ± SD; error bars represent SD in all figures. Intergroup comparisons were performed by two-tailed Student's t test. A p value $<0.05$ was considered to be statistically significant.

### Caspase 3/7 Assay and TUNEL Staining

For detection of apoptosis, we used the Caspase-Glo 3/7 Assay from Promega that measures caspase-3 and -7 activities because these members of the caspase family play important roles in apoptosis in mammalian cells. The measurements were done as described in the manufacturer manual. We used the In Situ Cell Death Detection Kit (Roche) according to the manufacturer's manual for TUNEL staining.

### Luciferase Assay

MzChA1 cells were transiently transfected with a cyclin E promotor luciferase reporter construct, a NICD expression construct, and phRL-TK (Promega) for normalization using FUGENE. After 48 hr, luciferase activity was measured using the "dual-luciferase reporter assay system" (Promega) following the manufacturer's instructions. In brief, cells were lysed in 1× passive lysis buffer; after 10 min, cells were scraped off the dishes and incubated for 5 min on ice. After centrifugation, 20 μl of cleared lysates were used for analysis of luciferase activity. The 96-well plate reader "Glomax-integrated luciferase technologies" (TURNER Biosystems) was used to quantify luciferase activity. Firefly luciferase activity was normalized to cotransfected Renilla luciferase activity (phRLTK).

## SUPPLEMENTAL INFORMATION

Supplemental Information includes four figures, one table, and Supplemental Experimental Procedures and can be found with this article online at http://dx.doi.org/10.1016/j.ccr.2013.04.019.

## ACKNOWLEDGMENTS

We thank Dr. Holly Sundberg Malek for critical advice. This work was supported by the DFG (Cluster of excellence, REBIRTH), SFB 738 and TR77, as well as the Emmy Noether Programme (ZE 545/2-1). We thank Warren S. Pear for dnMAML expression plasmid.

Received: October 31, 2010
Revised: June 11, 2012
Accepted: April 20, 2013
Published: May 30, 2013

## REFERENCES

Akhoondi, S., Sun, D., von der Lehr, N., Apostolidou, S., Klotz, K., Maljukova, A., Cepeda, D., Fiegl, H., Dafou, D., Marth, C., et al. (2007). FBXW7/hCDC4 is a general tumor suppressor in human cancer. Cancer Res. *67*, 9006–9012.

Benhamouche, S., Curto, M., Saotome, I., Gladden, A.B., Liu, C.H., Giovannini, M., and McClatchey, A.I. (2010). Nf2/Merlin controls progenitor homeostasis and tumorigenesis in the liver. Genes Dev. *24*, 1718–1730.

Cardinale, V., Carpino, G., Reid, L., Gaudio, E., and Alvaro, D. (2012). Multiple cells of origin in cholangiocarcinoma underlie biological, epidemiological and clinical heterogeneity. World J. Gastrointest. Oncol. *4*, 94–102.

Croquelois, A., Blindenbacher, A., Terracciano, L., Wang, X., Langer, I., Radtke, F., and Heim, M.H. (2005). Inducible inactivation of Notch1 causes nodular regenerative hyperplasia in mice. Hepatology *41*, 487–496.

El-Serag, H.B., Engels, E.A., Landgren, O., Chiao, E., Henderson, L., Amaratunge, H.C., and Giordano, T.P. (2009). Risk of hepatobiliary and pancreatic cancers after hepatitis C virus infection: A population-based study of U.S. veterans. Hepatology *49*, 116–123.

Fan, B., Malato, Y., Calvisi, D.F., Naqvi, S., Razumilava, N., Ribback, S., Gores, G.J., Dombrowski, F., Evert, M., Chen, X., and Willenbring, H. (2012). Cholangiocarcinomas can originate from hepatocytes in mice. J. Clin. Invest. *122*, 2911–2915.

Geisler, F., Nagl, F., Mazur, P.K., Lee, M., Zimber-Strobl, U., Strobl, L.J., Radtke, F., Schmid, R.M., and Siveke, J.T. (2008). Liver-specific inactivation of Notch2, but not Notch1, compromises intrahepatic bile duct development in mice. Hepatology *48*, 607–616.

Geng, Y., Eaton, E.N., Picón, M., Roberts, J.M., Lundberg, A.S., Gifford, A., Sardet, C., and Weinberg, R.A. (1996). Regulation of cyclin E transcription by E2Fs and retinoblastoma protein. Oncogene *12*, 1173–1180.

Hwang, H.C., and Clurman, B.E. (2005). Cyclin E in normal and neoplastic cell cycles. Oncogene *24*, 2776–2786.

Isomoto, H., Mott, J.L., Kobayashi, S., Werneburg, N.W., Bronk, S.F., Haan, S., and Gores, G.J. (2007). Sustained IL-6/STAT-3 signaling in cholangiocarcinoma cells due to SOCS-3 epigenetic silencing. Gastroenterology *132*, 384–396.

Kellendonk, C., Opherk, C., Anlag, K., Schütz, G., and Tronche, F. (2000). Hepatocyte-specific expression of Cre recombinase. Genesis *26*, 151–153.

Kim, H., Park, C., Han, K.H., Choi, J., Kim, Y.B., Kim, J.K., and Park, Y.N. (2004). Primary liver carcinoma of intermediate (hepatocyte-cholangiocyte) phenotype. J. Hepatol. *40*, 298–304.

Koch, U., and Radtke, F. (2007). Notch and cancer: a double-edged sword. Cell. Mol. Life Sci. *64*, 2746–2762.

Kodama, Y., Hijikata, M., Kageyama, R., Shimotohno, K., and Chiba, T. (2004). The role of notch signaling in the development of intrahepatic bile ducts. Gastroenterology *127*, 1775–1786.

Koepp, D.M., Schaefer, L.K., Ye, X., Keyomarsi, K., Chu, C., Harper, J.W., and Elledge, S.J. (2001). Phosphorylation-dependent ubiquitination of cyclin E by the SCFFbw7 ubiquitin ligase. Science *294*, 173–177.

Kossatz, U., Dietrich, N., Zender, L., Buer, J., Manns, M.P., and Malek, N.P. (2004). Skp2-dependent degradation of p27kip1 is essential for cell cycle progression. Genes Dev. *18*, 2602–2607.

Kossatz, U., Breuhahn, K., Wolf, B., Hardtke-Wolenski, M., Wilkens, L., Steinemann, D., Singer, S., Brass, F., Kubicka, S., Schlegelberger, B., et al. (2010). The cyclin E regulator cullin 3 prevents mouse hepatic progenitor cells from becoming tumor-initiating cells. J. Clin. Invest. *120*, 3820–3833.

Loeb, K.R., Kostner, H., Firpo, E., Norwood, T., D Tsuchiya, K., Clurman, B.E., and Roberts, J.M. (2005). A mouse model for cyclin E-dependent genetic instability and tumorigenesis. Cancer Cell *8*, 35–47.

Lorent, K., Yeo, S.Y., Oda, T., Chandrasekharappa, S., Chitnis, A., Matthews, R.P., and Pack, M. (2004). Inhibition of Jagged-mediated Notch signaling disrupts zebrafish biliary development and generates multi-organ defects compatible with an Alagille syndrome phenocopy. Development *131*, 5753–5766.

Malek, N.P., Sundberg, H., McGrew, S., Nakayama, K., Kyriakides, T.R., and Roberts, J.M. (2001). A mouse knock-in model exposes sequential proteolytic pathways that regulate p27Kip1 in G1 and S phase. Nature *413*, 323–327.

Murtaugh, L.C., Stanger, B.Z., Kwan, K.M., and Melton, D.A. (2003). Notch signaling controls multiple steps of pancreatic differentiation. Proc. Natl. Acad. Sci. USA *100*, 14920–14925.

Nakanuma, Y., Sato, Y., Harada, K., Sasaki, M., Xu, J., and Ikeda, H. (2010). Pathological classification of intrahepatic cholangiocarcinoma based on a new concept. World J. Hepatol. *2*, 419–427.

Patel, T. (2006). Cholangiocarcinoma. Nat. Clin. Pract. Gastroenterol. Hepatol. *3*, 33–42.

Ryan, M.J., Bales, C., Nelson, A., Gonzalez, D.M., Underkoffler, L., Segalov, M., Wilson-Rawls, J., Cole, S.E., Moran, J.L., Russo, P., et al. (2008). Bile duct proliferation in Jag1/fringe heterozygous mice identifies candidate modifiers of the Alagille syndrome hepatic phenotype. Hepatology *48*, 1989–1997.

Sansone, P., Storci, G., Tavolari, S., Guarnieri, T., Giovannini, C., Taffurelli, M., Ceccarelli, C., Santini, D., Paterini, P., Marcu, K.B., et al. (2007). IL-6 triggers malignant features in mammospheres from human ductal breast carcinoma and normal mammary gland. J. Clin. Invest. *117*, 3988–4002.

Satyanarayana, A., Wiemann, S.U., Buer, J., Lauber, J., Dittmar, K.E., Wüstefeld, T., Blasco, M.A., Manns, M.P., and Rudolph, K.L. (2003). Telomere shortening impairs organ regeneration by inhibiting cell cycle re-entry of a subpopulation of cells. EMBO J. *22*, 4003–4013.

Sekiya, S., and Suzuki, A. (2012). Intrahepatic cholangiocarcinoma can arise from Notch-mediated conversion of hepatocytes. J. Clin. Invest. *122*, 3914–3918.

Spruck, C.H., Won, K.A., and Reed, S.I. (1999). Deregulated cyclin E induces chromosome instability. Nature *401*, 297–300.

van Es, J.H., van Gijn, M.E., Riccio, O., van den Born, M., Vooijs, M., Begthel, H., Cozijnsen, M., Robine, S., Winton, D.J., Radtke, F., and Clevers, H. (2005). Notch/gamma-secretase inhibition turns proliferative cells in intestinal crypts and adenomas into goblet cells. Nature *435*, 959–963.

Villanueva, A., Alsinet, C., Yanger, K., Hoshida, Y., Zong, Y., Toffanin, S., Rodriguez-Carunchio, L., Sole, M., Thung, S., Stanger, B.Z., and Llovet, J.M. (2012). Notch signaling is activated in human hepatocellular carcinoma and induces tumor formation in mice. Gastroenterology *143*, 1660–1669.e7.

von Hahn, T., Ciesek, S., Wegener, G., Plentz, R.R., Weismüller, T.J., Wedemeyer, H., Manns, M.P., Greten, T.F., and Malek, N.P. (2011). Epidemiological trends in incidence and mortality of hepatobiliary cancers in Germany. Scand. J. Gastroenterol. *46*, 1092–1098.

Welcker, M., and Clurman, B.E. (2008). FBW7 ubiquitin ligase: a tumour suppressor at the crossroads of cell division, growth and differentiation. Nat. Rev. Cancer *8*, 83–93.

Welcker, M., Singer, J., Loeb, K.R., Grim, J., Bloecher, A., Gurien-West, M., Clurman, B.E., and Roberts, J.M. (2003). Multisite phosphorylation by Cdk2 and GSK3 controls cyclin E degradation. Mol. Cell *12*, 381–392.

West, J., Wood, H., Logan, R.F., Quinn, M., and Aithal, G.P. (2006). Trends in the incidence of primary liver and biliary tract cancers in England and Wales 1971-2001. Br. J. Cancer *94*, 1751–1758.

Xu, X., Kobayashi, S., Qiao, W., Li, C., Xiao, C., Radaeva, S., Stiles, B., Wang, R.H., Ohara, N., Yoshino, T., et al. (2006). Induction of intrahepatic cholangiocellular carcinoma by liver-specific disruption of Smad4 and Pten in mice. J. Clin. Invest. *116*, 1843–1852.

Zecchini, V., Domaschenz, R., Winton, D., and Jones, P. (2005). Notch signaling regulates the differentiation of post-mitotic intestinal epithelial cells. Genes Dev. *19*, 1686–1691.

Zender, L., Spector, M.S., Xue, W., Flemming, P., Cordon-Cardo, C., Silke, J., Fan, S.T., Luk, J.M., Wigler, M., Hannon, G.J., et al. (2006). Identification and validation of oncogenes in liver cancer using an integrative oncogenomic approach. Cell *125*, 1253–1267.

Zong, Y., Panikkar, A., Xu, J., Antoniou, A., Raynaud, P., Lemaigre, F., and Stanger, B.Z. (2009). Notch signaling controls liver development by regulating biliary differentiation. Development *136*, 1727–1739.

# Update

Cancer Cell

Volume 30, Issue 2, 8 August 2016, Page 353–356

DOI: https://doi.org/10.1016/j.ccell.2016.07.005

# A Critical Role for Notch Signaling in the Formation of Cholangiocellular Carcinomas

Steffen Zender, Irina Nickeleit, Torsten Wuestefeld, Inga Sörensen, Daniel Dauch, Przemyslaw Bozko, Mona El-Khatib, Robert Geffers, Hueseyin Bektas, Michael P. Manns, Achim Gossler, Ludwig Wilkens, Ruben Plentz, Lars Zender, and Nisar P. Malek*
*Correspondence: nisar.malek@med.uni-tuebingen.de
http://dx.doi.org/10.1016/j.ccell.2016.07.005

(Cancer Cell *23*, 784–795; June 10, 2013)

In the original article, which shows that the expression of Notch-ICD leads to the formation of intrahepatic cholangiocarcinomas, there is a duplication of actin blots in Figures 2G, 6F, and S2F.

Figure 2G shows the expression levels of cyclin E, cylin A, and p27 in wild-type and Notch-ICD mice undergoing liver regeneration after partial hepatectomy. The actin blot corresponding to the protein extracts from the wild-type mouse livers was duplicated and inadvertently used for the Notch-ICD mouse livers. The correct actin blot is now shown in the revised Figure 2G below.

In Figure 6F, the actin blot derived from Figure 6A, which shows that downregulation of Notch 1 by siRNA leads to a reduction of cyclin E levels, was erroneously duplicated in Figure 6F, which shows that inhibition of Notch activity by DAPT leads to cyclin E downregulation. In the revised Figure 6F shown below, the correct actin blot has been used.

Finally, in Figure S2F, the blot for cleaved Notch expression had been duplicated and erroneously labeled as Cyclin E. The correct cyclin E blot is now shown in the revised figure below.

While none of these errors affect the results or conclusions of this work, the authors would like to apologize for any confusion this might have caused.

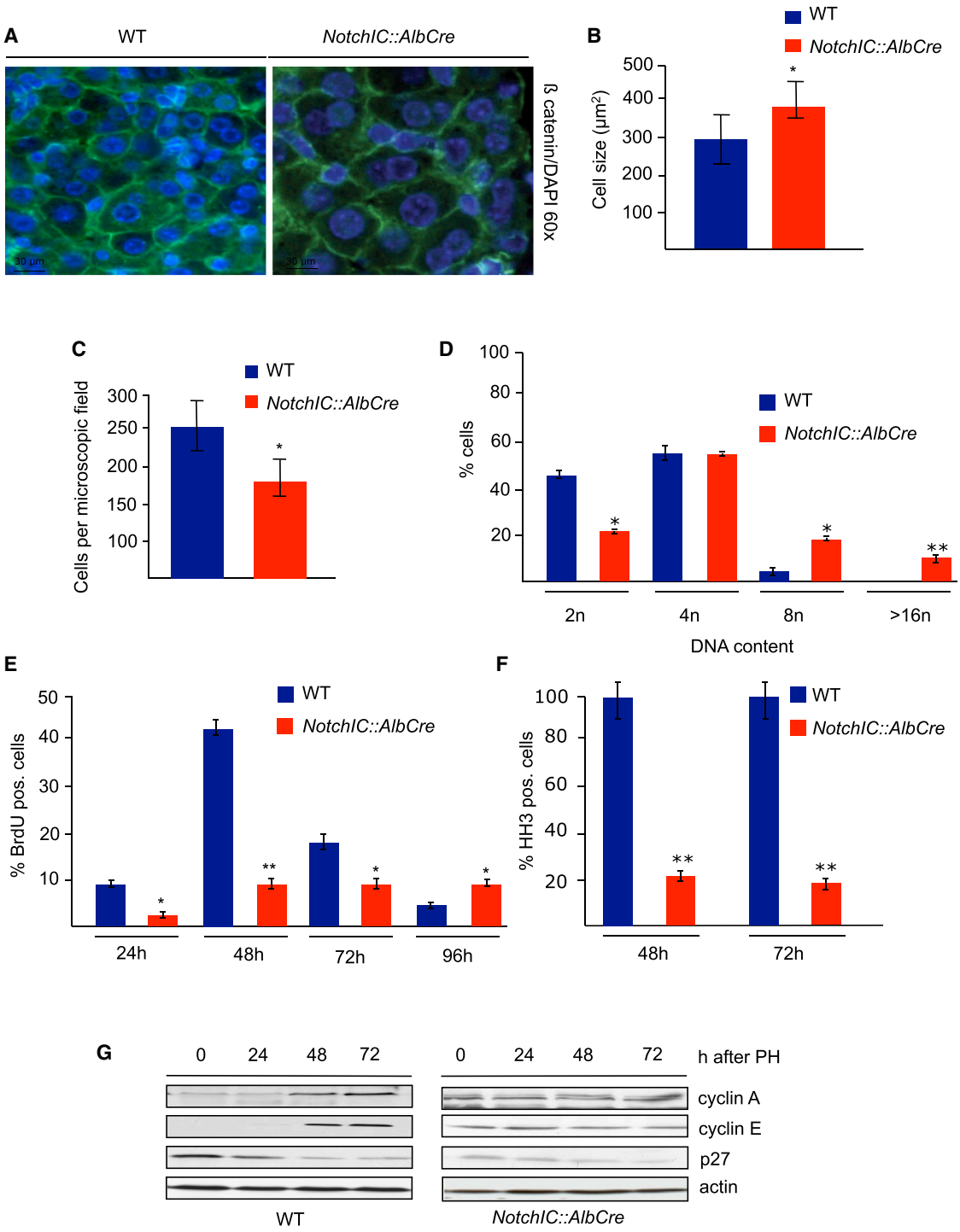


**Figure 2. Notch Signaling Leads to Dysregulated Expression of Cyclin E and Genetic Instability**

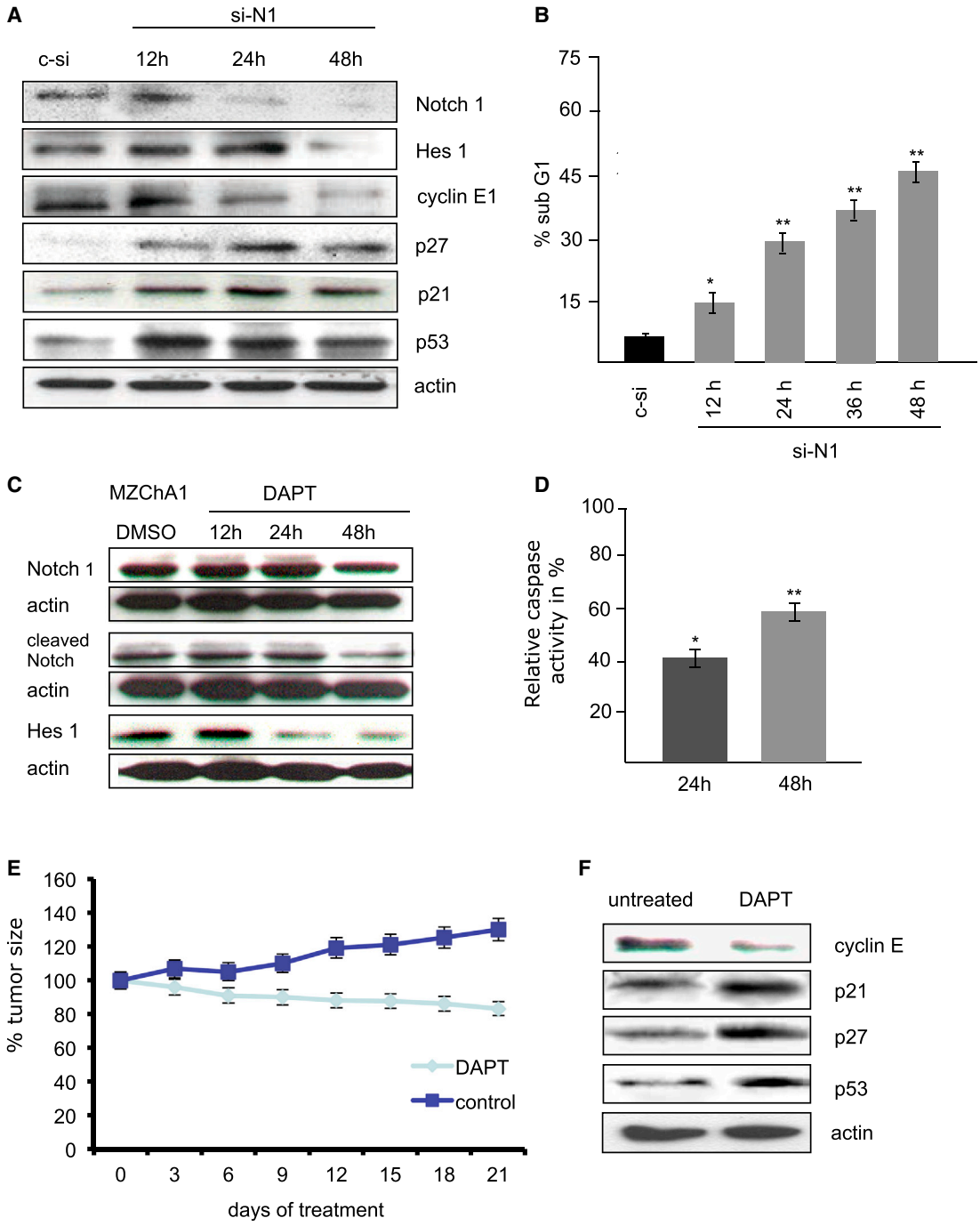


**Figure 6. Notch Signaling as a Therapeutic Target in CCC**

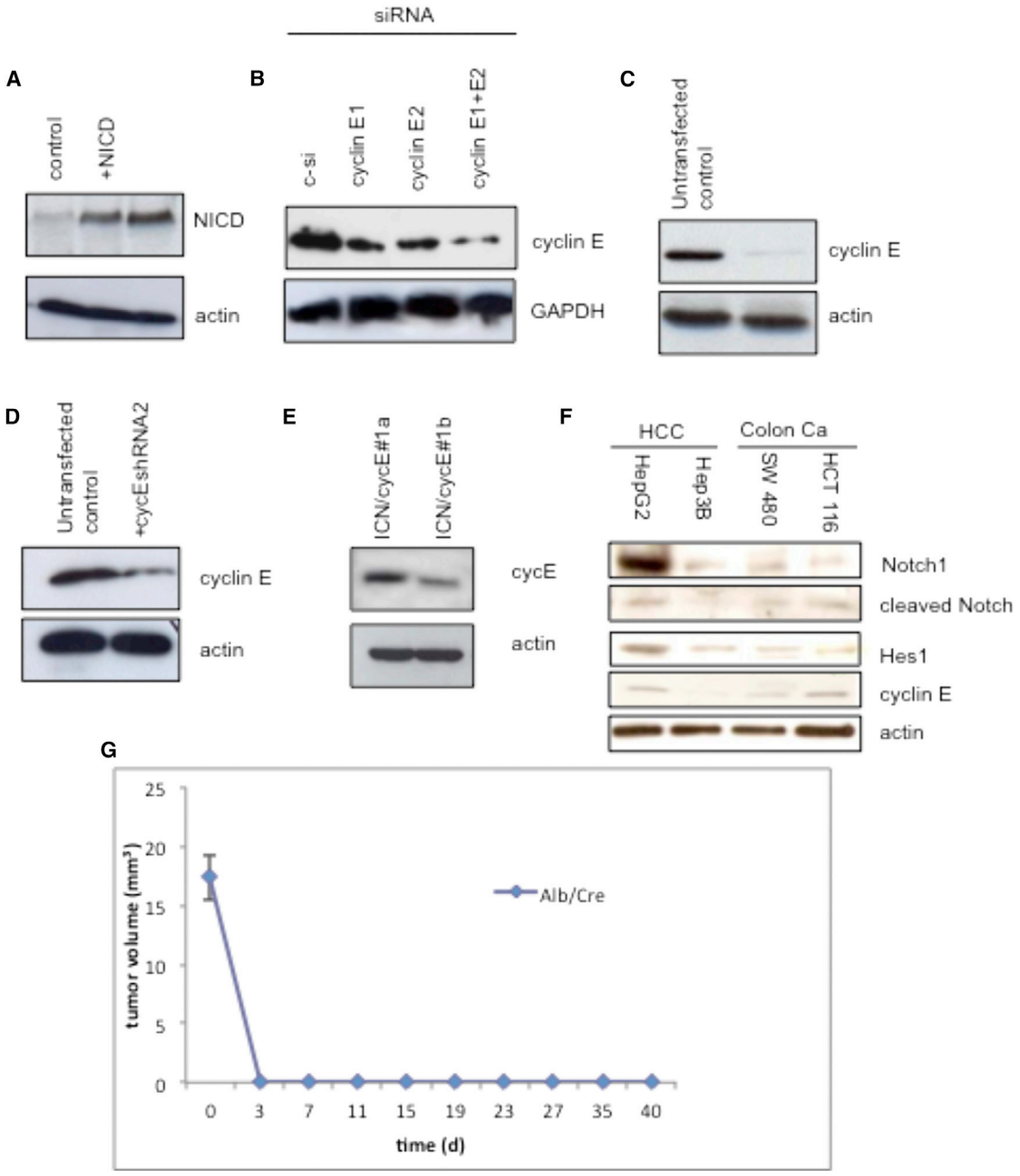
A
control
+NICD
NICD
actin
B
siRNA
c-si
cyclin E1
cyclin E2
cyclin E1+E2
cyclin E
GAPDH
C
Untransfected control
cyclin E
actin
D
Untransfected control
+cycEshRNA2
cyclin E
actin
E
ICN/cycE#1a
ICN/cycE#1b
cycE
actin
F
HCC
Colon Ca
HepG2
Hep3B
SW 480
HCT 116
Notch1
cleaved Notch
Hes1
cyclin E
actin
G
tumor volume (mm³)
25
20
15
10
5
0
0
3
7
11
15
19
23
27
35
40
time (d)
Alb/Cre

Figure S2